Redox Biology 48 (2021) 102176

Contents lists available at ScienceDirect

Redox Biology

journal homepage: www.elsevier.com/locate/redox

# Increased mitochondrial activity upon CatSper channel activation is required for mouse sperm capacitation

Juan J. Ferreira [c,d,1], Adriana Cassina [b,1], Pilar Irigoyen [a], Mariana Ford [a], Santiago Pietroroia [a], Nikita Peramsetty [c,d], Rafael Radi [b], Celia M. Santi [c,d,**], Rossana Sapiro [a,*]

[a] Departamento de Histología y Embriología and Centro de Investigaciones Biomédicas (CEINBIO), Facultad de Medicina UDELAR, Montevideo, Uruguay
[b] Departamento de Bioquímica and Centro de Investigaciones Biomédicas (CEINBIO) Facultad de Medicina, Universidad de la República, Montevideo, Uruguay
[c] Department of Obstetrics and Gynecology, Center for Reproductive Health Sciences, Washington University in St. Louis, School of Medicine, St. Louis, MO, United States
[d] Department of Neuroscience, Washington University in St. Louis, School of Medicine, St. Louis, MO, United States

ARTICLE INFO

*Keywords:*
Mitochondrial activity
CatSper channels
Spermatozoa capacitation
Fertilization
Hyperactivation
Calcium

ABSTRACT

To fertilize an oocyte, sperm must undergo several biochemical and functional changes known as capacitation. A key event in capacitation is calcium influx through the cation channel of sperm (CatSper). However, the molecular mechanisms of capacitation downstream of this calcium influx are not completely understood. Capacitation is also associated with an increase in mitochondrial oxygen consumption, and several lines of evidence indicate that regulated calcium entry into mitochondria increases the efficiency of oxidative respiration. Thus, we hypothesized that calcium influx through CatSper during capacitation increases mitochondrial calcium concentration and mitochondrial efficiency and thereby contributes to sperm hyperactivation and fertilization capacity. To test this hypothesis, we used high-resolution respirometry to measure mouse sperm mitochondrial activity. We also measured mitochondrial membrane potential, ATP/ADP exchange during capacitation, and mitochondrial calcium concentration in sperm from wild-type and CatSper knockout mice. We show that the increase in mitochondrial activity in capacitated wild-type sperm parallels the increase in mitochondrial calcium concentration. This effect is blunted in sperm from CatSper knockout mice. Importantly, these mechanisms are needed for optimal hyperactivation and fertilization in wild-type mice, as confirmed by using mitochondrial inhibitors. Thus, we describe a novel mechanism of sperm capacitation. This work contributes to our understanding of the role of mitochondria in sperm physiology and opens the possibility of new molecular targets for fertility treatments and male contraception.

## 1. Introduction

To fertilize an oocyte, sperm must undergo several biochemical and functional changes known as capacitation. During capacitation, sperm switch from progressive to hyperactivated motility and undergo a regulated release of acrosomal content in a process called the acrosome reaction (AR) [1,2]. These processes, which normally occur in the female reproductive tract, allow sperm to free themselves from the oviduct wall, penetrate the zona pellucida, and fuse with the oocyte. An important event controlling capacitation is an increase in intracellular [$Ca^{2+}$] [3] mediated by the cation sperm-specific channel (CatSper) [4,5]. *CatSper* Knockout (KO) mice are infertile because their sperm fail to hyperactivate and fertilize oocytes. However, the downstream effects of CatSper-mediated $Ca^{2+}$ increase in sperm have not been fully elucidated [6,7].

In other cell types, regulated $Ca^{2+}$ entry into mitochondria increases the efficiency of oxidative respiration [8,9] via activation of many $Ca^{2+}$-dependent mitochondrial enzymes resulting in the increase of ATP production [10]. Whether $Ca^{2+}$ plays similar roles in sperm mitochondria is unknown [11]. Complicating this picture is the unclear role of

* Corresponding author. Departamento de Histología y Embriología and Centro de Investigaciones Biomédicas (CEINBIO), Facultad de Medicina UDELAR, Montevideo, Uruguay.
** Corresponding author. Department of Obstetrics and Gynecology, Center for Reproductive Health Sciences, Washington University in St. Louis, School of Medicine, St. Louis, MO, United States.
*E-mail addresses:* Santic@wustl.edu (C.M. Santi), rsapiro@fmed.edu.uy (R. Sapiro).
[1] Both authors contributed equally to this work.

https://doi.org/10.1016/j.redox.2021.102176
Received 9 October 2021; Received in revised form 29 October 2021; Accepted 29 October 2021
Available online 1 November 2021

mitochondria in sperm capacitation. Although some data suggest that sperm rely on glycolysis instead of mitochondrial respiration to produce ATP for motility and fertilization [12], other studies showed that mitochondrial respiration increases during capacitation in both human [13,14] and mouse [35] sperm. However, the significance of this increase in mitochondrial activity during capacitation and its role in sperm hyperactivation, acrosome reaction (AR), and fertilization remains to be established.

Given that sperm from CatSper KO mice have reduced ATP production [15], we hypothesized that $Ca^{2+}$ influx through CatSper channels during capacitation enhances mitochondrial activity, thereby contributing to sperm hyperactivation and fertilization. To test our hypothesis, we studied mitochondrial activity using high-resolution respirometry (HRR), measurements of mitochondrial membrane potential (MMP) and evaluation of the ATP/ADP exchange during capacitation, as well as measurements of mitochondrial $Ca^{2+}$, both in wild-type and CatSper KO sperm. In addition, we analyzed the effects of mitochondrial function inhibitors on hallmark parameters of capacitation: AR, hyperactivation, tyrosine phosphorylation and the ability of the sperm to fertilize the egg.

## 2. Material and methods

### 2.1. Animals and ethics statement

All experimental procedures were approved by the Comisión Honoraria de Experimentación animal-CHEA,(Uruguay), or by the Animals studies committee of Washington University (St. Louis, MO,USA); and performed following the National Institute of Health Guide for the Care and Use of Laboratory Animals.

Animals were kept under a 12/12 h dark/light cycle at a constant temperature of 22 ± 2°C with free access to food and water. Wild-type sperm cells were obtained from male mice from two different strains, CB6F1/J mice (80–120 days old) in Montevideo-Uruguay and C57BL/6 male (60–90 days old) in Saint Louis, MO, USA. CatSper1 knock-out mice (CatSper KO) 60–90 days old were used in Saint Louis, MO, USA. Both were obtained from Jackson Laboratory. Acr-eGFP + Su9-Red2 transgenic mice (60-90 day-old) expressing green fluorescent protein (GFP) in the acrosome and red fluorescent protein (RFP) in the mitochondrial were obtained from Kelle Moley's laboratory, at Washington University in Saint Louis, School of Medicine, MO, USA. Oocytes were obtained from CB6F1/J female mice (4–8 weeks old), allocated in Montevideo-Uruguay. Mice were sacrificed via cervical dislocation.

### 2.2. Sperm collection and motility analysis

Motility analysis was performed in parallel in two laboratories. In Montevideo-Uruguay (UdelaR), sperm was collected from cauda epididymis in TYH media buffered with HEPES (NaCl 119.3 mM, KCl 4.7 mM, $CaCl_2.2H_2O$ 1.71 mM, $KH_2PO_4$ 1.2 mM, $MgSO_4.7H_2O$ 1.2 mM, $NaHCO_3$ 25.1 mM, Glucose 5.56 mM, Sodium pyruvate 0.51 mM, HEPES 10 mM, Phenol Red 0.0006%), supplemented with 4 mg/ml Bovine serum albumin and incubated for 60 min at 37 °C to induce capacitation. Sperm suspensions were loaded into pre-warmed sperm counting chambers (depth 20 μm) (DRM-600, Millennium Sciences, Inc. CELL-VU®, NY) and placed on a microscope stage at 37 °C. Sperm motility was examined using a Computer Assisted Semen Analysis (CASA) system (SCA6 Evolution, Microptic, Barcelona, Spain). The microscope used was Nikon (Japan) Eclipse E200 with phase contrast 100X equipped with Basler (Germany) acA780-75gc camera. The default settings included the following: frames acquired: 30; frame rate: 60 Hz; head size: 5–70 μm2. Sperm with hyperactivated motility were sorted using the following parameters: curvilinear velocity (VCL) > 182 μm/s and linearity coefficient (LIN) < 32%, Straightness (STR) > 57%. At least 500 sperm were analyzed in each experiment. In Saint Louis, MO, USA (Washington University) sperm was collected from cauda epididymis, incubated in non-Capacitated (NC) HS media buffered with HEPES (in mM: 135 NaCl, 5 KCl, 2 $CaCl_2$, 1 $MgSO_4$, 20 HEPES, 5 glucose, 10 lactic acid, 1 Na-pyruvate) at pH 7.4 for 15–20 min at 37 °C. After this time, the motile fraction of the sample was removed from the tube and split based on conditions to be tested. To achieve capacitation, sperm were incubated for 90 min at 37 °C in capacitated (CAP) HS medium with 5 mg/ml Bovine serum albumin (BSA), and 15 mM $NaHCO_3$ added. NC sperm were incubated for 90 °C at 37°C in HS without BSA and $NaHCO_3$ [55] . Drugs or inhibitors were added in NC or CAP HS media. For motility tests, 3 μl of the sample were placed into a 20 μm Leja standard count 4 chamber slide, pre-warmed at 37°C, and a minimum of 200 cells were counted. CASA analysis was performed with a Hamilton–Thorne digital image analyzer (HTR-CEROS II v.1.7; Hamilton–Thorne Research, Beverly, MA, United States). CASA settings used for the analysis were: objective Zeiss 10XNH; 30 frames were acquired at 60 Hz; camera exposure: 8 ms; camera gain: 300; integrated time: 500 ms; elongation max (%): 100; elongation min (%): 1; head brightness min 170; head size max: 50 $\mu m^2$; head size min: 5 $\mu m^2$; static tail filter: false; tail brightness min: 70; tail brightness auto offset: 8; tail brightness mode: manual; progressive STR (%): 80; progressive VAP (μm/s): 25. The criteria used to define hyperactivated sperm was: curvilinear velocity (VCL) > 150 μm/s, lateral head displacement (ALH) > 7.0 μm, and linearity coefficient (LIN) of 32%.

### 2.3. Acrosome reaction (AR) evaluation

AR status was evaluated both in NC and CAP sperm samples. Induced AR was obtained by incubating the cells with 10 μM of the calcium ionophore A23187 for 30 min prior the end of the capacitation process. Mitochondrial inhibitors were added to CAP media with and without A23187, and 2.5 μM Antimycin A (AA) (Sigma Aldrich, St. Louis, MO) or 2.5 μM Carbonyl cyanide-4-(trifluoromethoxy) phenylhydrazone (FCCP; Sigma-Aldrich). For all conditions 15 μl samples were placed onto glass slides, fixed in 4% paraformaldehyde for 30 min and washed twice with phosphate buffered saline (PBS). After washing, slides were incubated with 0.22% Coomassie stain (Coomassie Blue G-250; Thermo Scientific, Massachusetts), 50% methanol, 10% glacial acetic acid, 40% water for 2 min. Excess dye was removed by washing thoroughly using distilled water. Slides were air-dried and coverslips were placed on slides using mounting medium at room temperature. Stained sperm were examined under bright field microscopy at 400X (Nikon E100, Japan) to verify the percentage of sperm that had undergone AR. A minimum of 200 sperm was evaluated in each experiment.

### 2.4. In vitro fertilization (IVF) protocol

CB6F1/J female mice (4–8 weeks old) were super-ovulated using intraperitoneal administration of 5IU Pregnant Mare Serum Gonadotropin (PMSG) (Syntex, Argentina) followed by 5UI human Chorionic Gonadotropin (hCG) (Intervet, Netherlands) 48 h later. After 12–15 h of hCG injection, female mice were sacrificed, and the oocyte-cumulus complex was isolated in 250 ml of TYH-$CO_2$ buffered media (NaCl 119.3 mM, KCl 4.7 mM, $CaCl_2.2H_2O$ 1.71 mM, $KH_2PO_4$ 1.2 mM, $MgSO_4.7H_2O$ 1.2 mM, $NaHCO_3$ 25.1 mM, Glucose 5.56 mM, Sodium pyruvate 0.51 mM, Phenol red 0.0006%). Fertilization wells containing 30–50 eggs were inseminated with sperm (final concentration of $2.5 \times 10^6$ cells/ml) that had been CAP for 1 h in TYH-$CO_2$ buffered media supplemented with 4 mg/ml Bovine serum albumin at 37 °C and % $CO_2$ to induce capacitation, with or without mitochondria inhibitors (AA or FCCP) depending on the experimental conditions, washed twice by centrifugation, and resuspended in TYH-$CO_2$ media. After 3 h of insemination, eggs were washed and left in fresh media. To assess fertilization, eggs were evaluated after 24 h post-insemination, and two-cell stage embryos were counted.

### 2.5. High-resolution respirometry and respiration control ratio

Sperm cells oxygen consumption was determined by HRR [16]. HRR integrates highly sensitive oxygraphis (Oxygraph-2 K; Oroboros Instruments GmbH, Innsbruck, Austria) with software (DatLab, version 4.2; Oroboros Instruments GmbH) that presents respiration in terms of oxygen rate (pmol $O_2/10^6$ cells/sec). Basal oxygen consumption was measured for 10 min, then 2 μg/ml Oligomycin (Sigma-Aldrich, St. Louis, MO) were added to the chamber to block mitochondrial ATP synthase. Maximal respiration was obtained by subsequent 0.5 μM stepwise of FCCP. Finally, 2.5 μM Antimycin A (Sigma-Aldrich) was added to distinguish mitochondrial from residual (non-mitochondrial respiration) oxygen consumption. A total of 15 million sperms cells/ml per condition were evaluated. Stirring speed was set to 750 rpm. For each sperm sample (Fig. 1A), we measured mitochondrial basal respiration rate. By subtracting the oligomycin-resistant respiration rate from the basal respiration rate, we calculated the oxygen consumption rate linked to ATP synthesis. We also measured maximal respiration rate in the presence of FCCP. Finally, we measured the non-mitochondrial respiration rate, which we subtracted from all the other values. From these measurements, we calculated 1) Coupling efficiency = ratio between respiration linked to ATP synthesis and basal respiration [1–2/1], 2) RCR = ratio between maximal and oligomycin-resistant respiration rates [3/2], and 3) spare respiratory capacity = ratio between the maximal and basal respiration rates) [3/1]. It is important to note that the resulting values were internally normalized in each sample, and they were independent of cell number, protein mass, and viability. It is also important to notice that the cell's respiration inhibited by oligomycin in intact cells is comparable to isolated mitochondria state 4 oligomycin (in the presence of substrate plus ADP plus oligomycin). The maximal respiration rate caused by the addition of the uncoupler FCCP to intact cells is comparable to state 3 ADP of isolated mitochondria in presence of an excess of substrate plus ADP [17].

### 2.6. Mitochondrial membrane potential measurements

Flow cytometry: Sperm collected from cauda epididymis was allowed to swim-out in TYH media CAP media, buffered with HEPES, for 5–10 min. Tissue was extracted and the suspended cells were split into two samples with a final concentration of 106 cells/ml. One of the samples was treated immediately for 25 min at 37°C with 300 nmol/L of lipophilic cationic dye tetramethyl rhodamine methyl ester perchlorate (TMRM) (Sigma-Aldrich Inc., St Louis, MO, USA) and was considered as our (control) NC condition. The second sample was incubated for 90 min at 37°C and 5% $CO_2$ to induce capacitation, and TMRM was added 25 min before finishing the incubation period. TMRM was washed from both conditions by centrifuging the samples at 400 g and resuspended in 400 ml of PBS. Half of the washed sample (500 μl) was analyzed by flow cytometry and the remaining (500 μl) was incubated with 20 μM FCCP for 15 min and analyzed. Values obtained with FCCP were used as $F_{min}$ to normalize the sample's fluorescence. We used the Geo Mean fluorescence values of FCCP at each experiment as minimum fluorescence to normalized fluorescence of M1 and M2 and discard differences related to the loading of TMRM for each experiment.

Flow cytometry analysis was performed using a FACS Calibur flow cytometer (Becton Dickinson, San Jose, CA). Cellular size and granularity were analyzed in the forward and side scatter (FSC–H and SSC-H), respectively. For each sample, 30000 single events were recorded in the forward light scatter/side light scatter dot plot. A gate was used to separate sperm from debris. TMRM was detected using a 585/42 nm bandwidth filter (FL-2). Samples were analyzed with Cell Quest software. Two populations of cells (M1 and M2, Fig. 1-C) with different MMP were consistently obtained. We analyzed the population with higher MMP (M2) based on several factors: 1) MMP measurements after capacitation for both populations made in our laboratory, 2) previously described methodology by Uribe P. et al. [18], and 3) similar results published using TMRM in sperm by Yang Q. et al. [19] . See Supplementary Fig. 1, for analysis of M1 population.

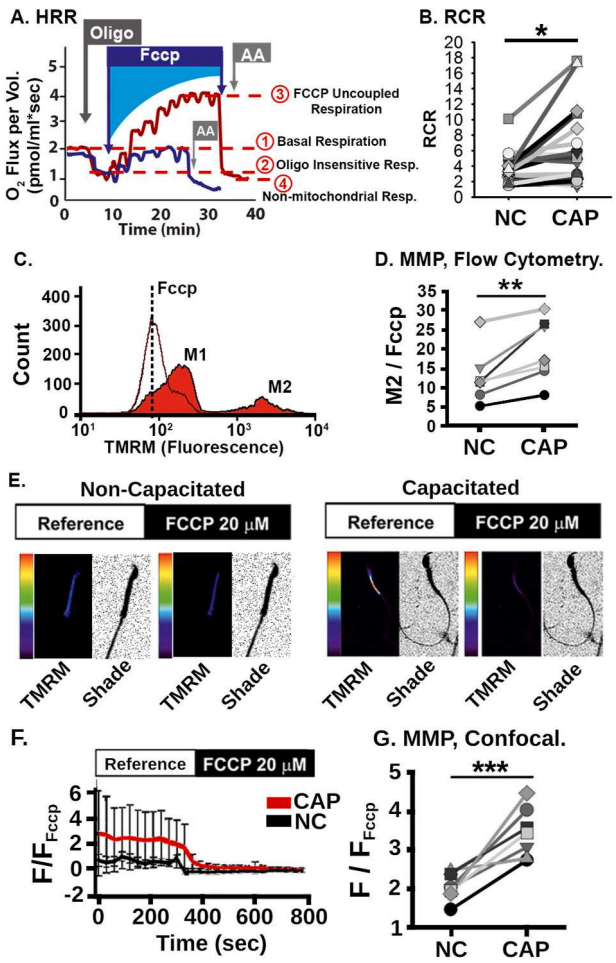


**Fig. 1. Capacitated sperm exhibit increased mitochondrial function. A.** Representative trace of oxygen consumption rate from CAP mouse sperm (red line) and NC (blue line). Dotted lines show representative respirometry parameters in CAP condition. Sperm cells were exposed sequentially to oligomycin (oligo), Carbonyl cyanide 4-(trifluoromethoxy) phenylhydrazone (FCCP), and Antimycin A (AA). **B.** Respiratory Control Ratio (RCR) values measured from wild-type CAP and NC sperm (n = 21). **C.** Representative histograms of TMRM fluorescence from CAP sperm, recorded with flow cytometry. **D.** Graph shows normalized TMRM fluorescence values (MMP) of M2 cell population under NC and CAP conditions (n = 7). See Supplementary Fig. 1, for analysis of M1 population. E. Representative confocal images of Wild-type sperm loaded TMRM before and after application of FCCP, under NC (left) and CAP (right). TMRM images shows the fluorescence obtained under the same technical specifications measured under NC (left) and CAP (right) conditions. Shade images represent the shape of the sperm cell used. Color bars represent color code for the gray scale from 0 to 255. Fluorescence was measured only in the sperm midpiece, and only cells responding to FCCP were included in the measurements. **F.** Representative normalized traces of TMRM fluorescence from NC and CAP sperm. Fluorescence was measured only in the sperm midpiece. Only cells responding to FCCP were included in the measurements. **G.** Graphs show normalized TMRM sperm midpiece fluorescence for NC and CAP sperm samples (n = 8). For **B** and **D**. paired *t-test* was used to determine statistical significance and an independent *t-test* was used in G. *p < 0.05 and ***p < 0.001. (n) represents the number of animals. (For interpretation of the references to color in this figure legend, the reader is referred to the Web version of this article.)

Single Cell MMP measurements by Confocal Imaging: Sperm cells were collected from cauda epididymis. Sperm were obtained by Swim-out in HS NC or CAP media for 10–15 min. NC samples were incubated in NC HS media, and CAP samples in CAP HS media, for 90 min at

37°C. At 60 min of incubation 200–300 nmol/L TMRM was added to all conditions and incubated for 30 min at 37°C. TMRM was washed from all samples by centrifugation and cells were resuspended in NC HS media and allowed to attach for 5–10 min to Poly-L-lysine (0.1%)-coated coverslips. Basal TMRM fluorescence for all the different conditions was measured before the addition of 20 μM FCCP, which was used to determine $F_{min}$ and to normalize basal fluorescence values.

Fluorescence values from different animals and different conditions were adjusted to the same laser intensity and gain voltage. Recordings were performed with a confocal microscope (Leica SP8) and LAS X 3.5.2.18963 software equipped with an ACS APO 40x, 1.15 Numerical aperture objective, and oil-immersion objective. The parameters for the acquisition were: "xyt" images, 1024 x 1024 pixels, pixel size 0.269 μm, pinhole of 600.0 μm, 400 Hz unidirectional sampling, frames were obtained every 30 s. Excitation was performed by 543-nm laser and emitted fluorescence was measured at 556 nm–600 nm. All experiments were performed at room temperature (22–23°C). Fluorescence was measured only in regions of interest (ROI) corresponding to the sperm midpiece, using ImageJ software (version 1.48). Data was analyzed using pclamp 10 and Sigmaplot 12.

### 2.7. Fluo-5N and mitochondrial markers co-localization images

Sperm from wild-type mice (C57Bl6) or Acr-eGFP + Su9-Red2 transgenic mice were collected by swim-up in HS media, loaded with 2–4 μM Fluo-5N cell permeant AM-ester (Fluo-5N AM or Fluo-5N), and incubated with 200 nM MitoTracker® Red CMXRos – M7512 (Invitrogen, USA). To load Fluo-5N, cells were incubated at 37°C for 45–60 min in HS with 2 μM Fluo-5N AM and 0.05–0.1% Pluronic Acid F-127. MitoTracker was added 20–30 min before the Fluo-5N loading was finished. Sperm were then centrifuged, resuspended in HS NC media, and allowed to attach for 5–10 min to Poly-L-lysine (0.1%)- coated coverslips. Images were acquired using a confocal microscope (Leica SP8) and LAS X 3.5.2.18963 software equipped with an ACS APO 63x, 1.15 Numerical aperture objective, oil-immersion objective. Images's dimensions were 2048 x 2048 pixels. Sperm were excited at 488 nm and 543 nm and emitted fluorescence was measured at 500–530 and > 560 nm, for Fluo-5N and MitoTracker respectively. All experiments were performed at room temperature (22–23°C). ImageJ software (version 1.48) was used to analyze the images.

### 2.8. Mitochondrial $Ca^{2+}$ measurements

After swim-up in HS NC or CAP media, motile cells were incubated with 2–4 μM Fluo-5N AM and 0.05% Pluronic F-127 at 37°C for 60–90 min. After loading, sperm cells were centrifuged at 1500–2000 rpm for 5–10 min and resuspended in the corresponding media. Sperm were allow to attach to Poly-L-lysine (0.1%) coated coverslips placed on the recording chamber's floor for 5 min. A local perfusion device with an estimate exchange time of 10 s was used to apply various test solutions. Calcium signals were recorded with a Leica AF 6000LX system with a Leica DMi8000 inverted microscope, equipped with a 63X objective (HC PL FluoTar L 63X/0.70 Dry) air objective and an Andor-Zyla-VCS04494 camera. An halogen lamp was used with a 488 ± 20 nm excitation filter and a 530 ± 20 nm emission filter. Data was collected with Leica LasX 2.0.014332 software. Acquisition parameters were: 20 ms exposure time, 4x4 binning, 1024 x 1024 pixels resolution. Whole images were collected every 10 s. LAS X, ImageJ, Clampfit 10 (Molecular Devices), and SigmaPlot 12 were used to analyze data.

ROI were selected in the sperm midpiece. Reference Fluo-5N fluorescence was measured at the beginning of the experiments ($F_{Ref}$), for all the conditions. To compare $F_{Ref}$ levels across different animals and experimental conditions, we normalized Fluo-5N fluorescence using $F_{min}$ and $F_{max}$ obtained from each cell. $F_{min}$ was obtained by perfusing cells with 0 mM $Ca^{2+}$ + 2 mM EGTA and 2–5 μM Ionomycin. $F_{max}$ was obtained by perfusing the cells with 2 mM $Ca^{2+}$ + 2–5 μM Ionomycin. Experiments were performed at room temperature.

### 2.9. Statistical analysis

Sigmaplot version 12.0 (Systat Software Inc.), and GraphPad Prism version 6.01 for Windows (GraphPad Software, La Jolla California USA http://www.graphpad.com) were used for all statistical analysis. An unpaired Student's t-test was used to compare independent samples, and a paired *t*-test was used to compare data in studies performed in the same sample. Data are expressed as the mean ± SD. P-value < 0.05 was considered statistically significant.

## 3. Results

### 3.1. Mitochondrial respiration increases in capacitated mouse sperm

High-resolution respirometry (HRR) was performed in non-capacitated (NC) and capacitated (CAP) sperm. Fig. 1A shows a representative trace of oxygen consumption rate measured in capacitated sperm. The mean respiratory control ratios (RCR) (5.8 Mean ± 4.8 SD vs. 3.5 Mean ± 1.9 SD) and coupling efficiency (0.56 Mean ± 0.20 SD vs. 0.48 Mean ± 0.18 SD) were both significantly higher in CAP than in NC sperm (Fig. 1B and Table 1). We found no significant difference in spare respiratory capacity. We next measured MMP in NC or CAP sperm with the dye TMRM [18,20]. By flow cytometry we detected two sperm populations (M1 and M2, Fig. 1C) with different MMP in both NC and CAP sperm. Similar populations have been reported previously in human sperm [18]. We found that the normalized fluorescence of the M2 population was significantly higher in CAP sperm than in NC sperm (13.22 Mean ± 6.6 SD vs. 8.83 Mean ± 7.80 SD, n = 7, Fig. 1D). In addition, the M2 peak was completely abolished upon addition of the uncoupling agent carbonyl cyanide 4-(trifluoromethoxy) phenylhydrazone (FCCP) in both NC and CAP sperm. These data suggest that MMP in the M2 population increases during capacitation. We also used confocal imaging to measure TMRM fluorescence in the midpiece of individual NC and CAP sperm (see Fig. 1E and F for a representative example), we found that TMRM fluorescence was significantly higher in CAP than in NC sperm (3.27 Mean ± 0.50 SD vs. 2.05 Mean ± 0.36 SD, Fig. 1G). Taken together, these data reveal that mitochondrial activity is higher CAP than in NC sperm.

### 3.2. Mitochondrial respiration during capacitation is important for hyperactivated motility and oocyte fertilization

To address whether mitochondrial activity was required for the functional hallmarks of capacitation, we capacitated sperm for 1 h in control conditions or in the presence of FCCP or AA. A significantly higher percentage of sperm were hyperactivated in control conditions than in the presence of FCCP or AA (20.43 Mean ± 9.89 SD, n = 15, vs. 10.51 Mean ± 8.44 SD, n = 15, vs. Mean 7.58 ± 7.76 SD, n = 11, Fig. 2A). In contrast, FCCP and AA had no effect on the percentage of sperm that underwent spontaneous or induced AR (Fig. 2B). Additionally, AA had no effect on protein tyrosine phosphorylation (Supplementary Fig. 2). Sperm treated with FCCP or AA were significantly less able to fertilize oocytes than untreated sperm (Fig. 2C) Fig. 2D shows a representative in vitro fertilization control experiment (without any mitochondrial inhibitors) at 2-cell stage embryo.

Together, these data indicate that while mitochondrial activity during capacitation is not required for the AR or tyrosine phosphorylation, it significantly contributes to sperm hyperactivation and, notably, to their ability to fertilize oocytes.

### 3.3. Mitochondrial respiration is impaired in sperm from CatSper knockout (KO) mice

By analyzing HRR in sperm from CatSper KO mice we found that

**Table 1**
Oximetry values in NC and CAP sperm from wild-type and CatSper KO mice. Coupling efficiency = Oligomycin-sensitive respiration/basal respiration; RCR = Maximal respiration in the presence of FCCP/ATP turnover; spare respiratory capacity = Maximal respiration in the presence of FCCP/Basal Respiration.

| Index | | Wild-type | | | | CatSper KO | | |
|---|---|---|---|---|---|---|---|---|
| | | Mean | SD | P-Value | | Mean | SD | p-value |
| **Coupling efficiency** | **NC** | 0.48 | 0.18 | **0.009** | **NC** | 0.37 | 0.06 | **0.1** |
| | **CAP** | 0.56 | 0.20 | | **CAP** | 0.32 | 0.11 | |
| **RCR** | **NC** | 3.5 | 1.9 | **0.012** | **NC** | 2.12 | 0.50 | **0.84** |
| | **CAP** | 5.8 | 4.8 | | **CAP** | 2.05 | 0.70 | |
| **Spare Respiration Capacity** | **NC** | 1.5 | 0.8 | **0.96** | **NC** | 1.34 | 0.36 | **0.72** |
| | **CAP** | 1.5 | 0.9 | | **CAP** | 1.43 | 0.61 | |

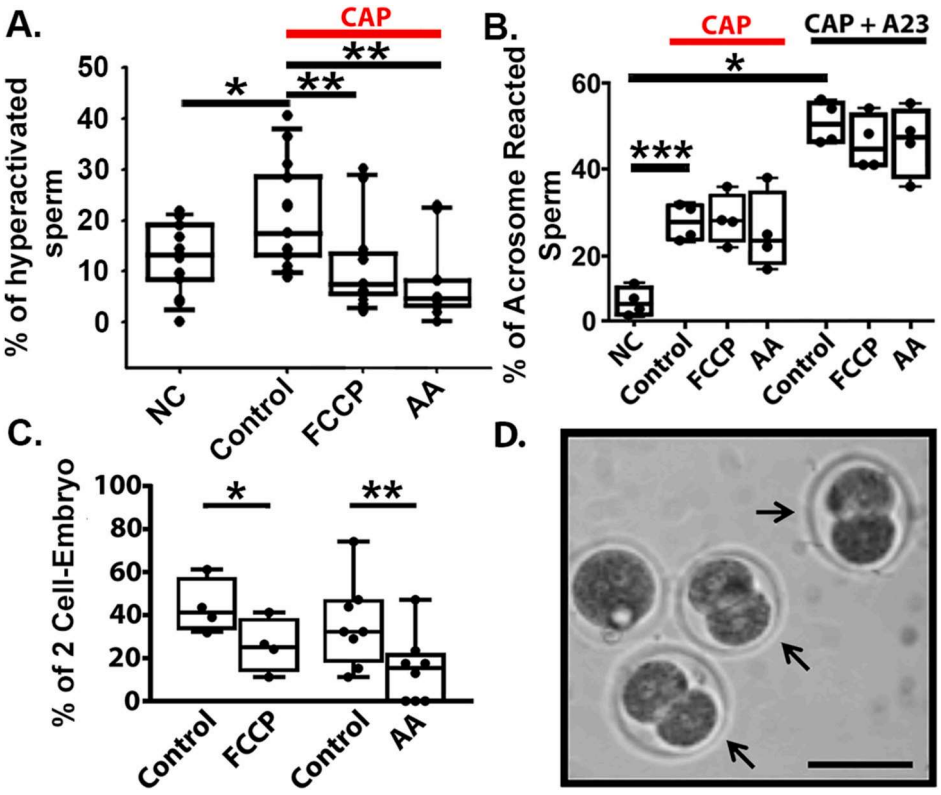


**Fig. 2. Mitochondrial inhibitors impair mouse sperm capacitation and *in vitro* fertilization. A.** Hyperactivation measurements obtained by CASA from CAP sperm in control conditions and in the presence of FCCP and AA. **B.** Spontaneous AR and A23187-induced AR from NC, CAP control, and CAP with FCCP or AA. **C.** Percentage of oocytes that reached the 2-cells stage embryo after 24 h of sperm addition. Graph shows mean ± SD. **D.** Representative phase contrast image of the 2-cell embryo stage (arrows) from experiment C under control conditions. Bar represents a 50 μm scale. To determine statistical significance between the groups, independent *t-test* were used on A and B, and Paired *t-test* was used in C. *p < 0.05, **p < 0.01, and ***p < 0.001 respectively. In A and C dots black represents the number of animals while in C represents each trial.

respiration values in sperm from CatSper KO mice did not differ between NC and CAP conditions (Fig. 3 A, B and Table 1). The MMP showed no statistical difference between CAP and NC in CatSper KO mice (2.90 Mean ± 0.92 SD vs. 3.10 Mean ± 0.48 SD, $P = 0.746$, Fig. 3C and D). Fig. 3E shows the variation in MMP after CAP for wild-type and CatSper KO mice; MMP increase in wild-type sperm during capacitation is statistically larger than in the KO sperm. Our results indicate that CatSper is involved in increasing sperm mitochondrial activity during capacitation.

### 3.4. *Mitochondrial $Ca^{2+}$ concentration increases during capacitation in sperm from wild-type but not CatSper KO mice*

We next wanted to test whether the CatSper-dependent increase in cytoplasmic [$Ca^{2+}$] during capacitation (Supplementary Fig. 3) leads to an increase in mitochondrial [$Ca^{2+}$]. To do so, we developed a new method to measure mitochondrial [$Ca^{2+}$] in mouse sperm by using the fluorescent $Ca^{2+}$-indicator, Fluo-5N. Whereas Fluo-4 measures [$Ca^{2+}$] in the 100 nM–300 nM range and is suitable for measuring cytoplasmic [$Ca^{2+}$], Fluo-5N has a lower $Ca^{2+}$-binding affinity and is suitable for measuring [$Ca^{2+}$] in the 1 μM to 1 mM range, appropriate for measuring [$Ca^{2+}$] in mitochondria [21]. We first confirmed that Fluo-5N co-localized in the sperm midpiece with mitochondrial markers. In sperm from Acr-eGFP + Su9-Red2 transgenic mice, which express green fluorescent protein (GFP) in the acrosome and red fluorescent protein in mitochondria (RFP), Fluo-5N co-localized with RFP in the sperm midpiece (Supplementary Figs. 4A and E). Likewise, Fluo-5N co-localized with MitoTracker® red in the sperm midpiece (Supplementary Figs. 4B and E). In contrast, Fluo-4 distributed throughout the entire sperm (Supplementary Figs. 4C and E). Although Fluo-5N was also detected in the acrosome (Supplementary Figs. 4A and E), we excluded this in our assays by only measuring fluorescence in the sperm midpiece. Combined fluorescence profiles of the midpiece labeled with the different fluorophores are shown in Supplementary Fig. 4F. While RFP and MitoTracker® red fluorescence curves completely overlap with Fluo-5N profile in mitochondria, the overlay with Fluo- 4 is partial, which indicates that neither RFP nor Mitotracker colocalize with Fluo-4 AM in the cytoplasm (supplementary 4). To further confirm that our assay measured mitochondrial [$Ca^{2+}$], we loaded sperm with either Fluo-5N or Fluo-4 and continuously measured fluorescence in the midpiece before and after adding FCCP (Supplementary Fig. 5A). As expected, Fluo-5N fluorescence decreased in the midpiece upon addition of FCCP (Supplementary Fig. 5B), whereas Fluo-4 fluorescence in the midpiece increased (Supplementary Fig. 5C), suggesting that FCCP caused $Ca^{2+}$ to be released from the mitochondria into the cytosol. Thus, we concluded

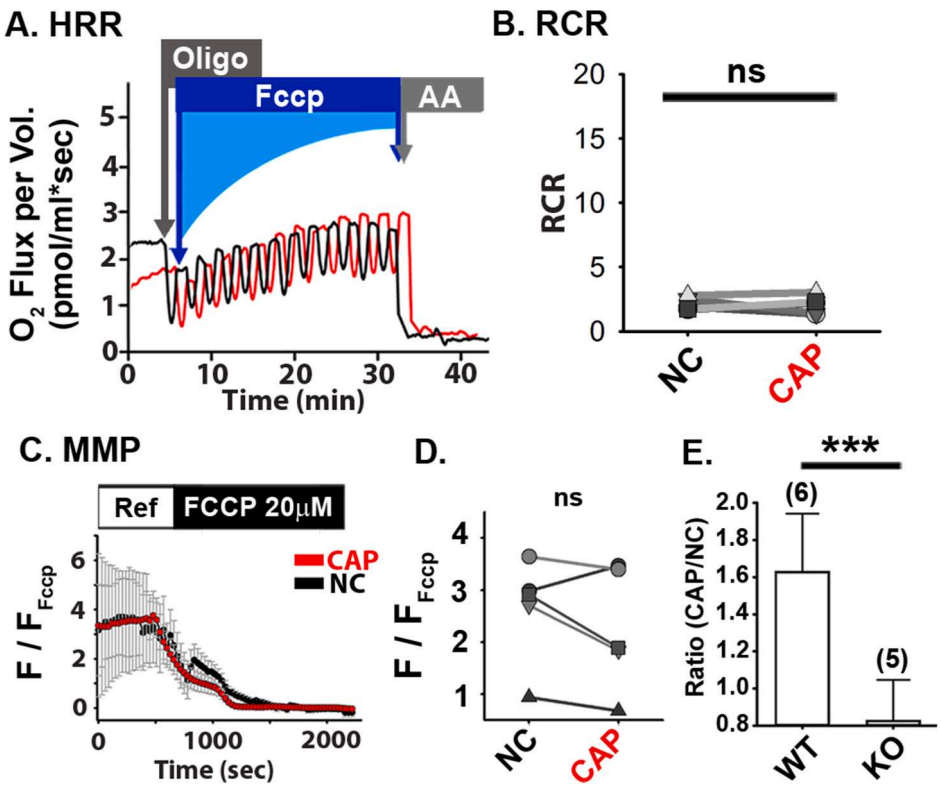


**Fig. 3. CatSper KO sperm lacks capacitation-induced mitochondrial function increase. A.** Representative recordings of a HRR from CAP (red line), and NC (black line) in CatSper KO sperm. Oxygen consumption was measured in control conditions and after the addition of mitochondrial inhibitors, Oligomycin, FCCP and AA. **B.** Respiratory control ratio (RCR) measurements from CAP and NC CatSper KO mouse sperm. A paired *t-test* was used to determine statistical significance (n = 5). **C.** Paired representative traces of normalized TMRM fluorescence, under CAP and NC conditions. **D.** Graph shows normalized TMRM fluorescence under NC and CAP conditions (n = 5). **E.** TMRM fluorescence ratio after CAP (normalized to NC) in wild-type and CatSper KO mice. To determine statistical significance, paired *t-test* was used. ns $p > 0.050$ and ***$p < 0.001$. Error bars represent SD. (n) represents the number of animals. (For interpretation of the references to color in this figure legend, the reader is referred to the Web version of this article.)

that our method accurately measured [$Ca^{2+}$] of the mitochondria in the sperm midpiece.

We then applied this method to determine if mitochondrial $Ca^{2+}$ content was different between NC and CAP wild-type sperm. Fig. 4A shows representative images of CAP wild-type sperm loaded with Fluo-5N. At 2 mM extracellular [$Ca^{2+}$], we observed that mitochondrial $Ca^{2+}$ was higher in CAP than in NC wild-type sperm (Fig. 4B and D). In contrast, when we performed the experiment at 0 mM extracellular [$Ca^{2+}$], we observed no difference in mitochondrial $Ca^{2+}$ content between CAP and NC wild-type sperm (Fig. 4B and D). This is an expected result, as capacitation does not occur in the absence of extracellular calcium.

We found that mitochondrial $Ca^{2+}$ content increased with higher extracellular [$Ca^{2+}$] (0, 0.5,1 and 2 mM) in both NC and CAP wild-type sperm, however, the increase was significantly larger in CAP sperm (Fig. 4D, Table 2). Whereas mitochondrial Fluo-5N fluorescence reached a plateau at 1 mM extracellular $Ca^{2+}$ in NC sperm, the Fluo-5N fluorescence further increased at 2 mM extracellular $Ca^{2+}$ in CAP sperm, consistently with the extracellular [$Ca^{2+}$] reported to achieve capacitation [22].

We conclude that mitochondrial [$Ca^{2+}$] depends on extracellular [$Ca^{2+}$]. Importantly, mitochondrial [$Ca^{2+}$] are significantly higher in CAP than in NC wild-type sperm. To determine whether the increase in mitochondrial [$Ca^{2+}$] in CAP sperm was dependent on CatSper activity; we measured changes in mitochondrial [$Ca^{2+}$] during capacitation in sperm from CatSper KO mice. Our results showed that in CatSper KO sperm, at 2 mM extracellular [$Ca^{2+}$], there is no difference in Fluo-5N fluorescence of the midpiece between NC and CAP conditions (Fig. 4C). When we plotted values of fluorescence in the midpiece of sperm from CatSper KO mice, we found that mitochondrial [$Ca^{2+}$] only increased when we changed extracellular [$Ca^{2+}$] from 0 to 0.5 mM, and then it remained constant. This increase was similar in NC and CAP sperm (Fig. 4E). The fact that $Ca^{2+}$ increased at all in response to increased extracellular [$Ca^{2+}$] in sperm from CatSper KO mice suggests that $Ca^{2+}$ can enter sperm through another pathway. Consistent with this idea, $Ca^{2+}$ measurements obtained with the ratiometric dye Fura 2 a.m. showed that the cytosolic [$Ca^{2+}$] of CatSper KO sperm was 90–100 nM (Supplementary Fig. 3**).** Nonetheless, mitochondrial [$Ca^{2+}$] was significantly lower in CAP sperm from CatSper KO mice than in CAP sperm from wild-type mice (Fig. 4D and E and Table 2).

Another way to validate that CatSper channels were involved in the increased mitochondrial [$Ca^{2+}$], was to treat sperm from wild-type mice with the CatSper channel blocker Mibefradil during capacitation. Mibefradil (20 μM) significantly reduced the increase of mitochondrial [$Ca^{2+}$] associated with capacitation (Supplementary Fig. 6). Taken together these results confirmed that mitochondrial [$Ca^{2+}$] increase involved CatSper activation. This pharmacological approach confirms that the absence of CatSper conductance is uniquely responsible for the calcium defects that we have seen in the CatSper KO and rules out potential pleiotropic effects of the CatSper gene knock out (Supplementary Fig. 5).

### 3.5. *Increase in mitochondrial function associated with capacitation depends on the mitochondrial $Ca^{2+}$ uniporter (MCU)*

We suspected that the increase of mitochondrial [$Ca^{2+}$] in CAP sperm occurred via $Ca^{2+}$ influx through the MCU, which resides in the internal mitochondrial membrane [23]. To test this idea, we treated sperm with the specific MCU inhibitor Ru360 during capacitation [24], and then measured capacitation-associated changes in mitochondrial [$Ca^{2+}$], MMP, and sperm hyperactivation.

First, we found that mitochondrial [$Ca^{2+}$] was significantly reduced after capacitation in the presence of Ru360 when compared with those without Ru360 (Fig. 5A and B and Table 3). Second, we treated CAP sperm with vehicle or Ru360, loaded them with TMRM in the presence of 2 mM extracellular $Ca^{2+}$, and used our confocal microscopy assay to measure MMP. The normalized TMRM fluorescence was lower in sperm treated with Ru360 than in those without Ru360 (1.789 Mean ± 0.717 SD vs. 3.00 Mean ± 0.43 SD, P = 0.027, Fig. 5C). Moreover, whereas the MMP was 60% higher in CAP than NC sperm treated with vehicle, the

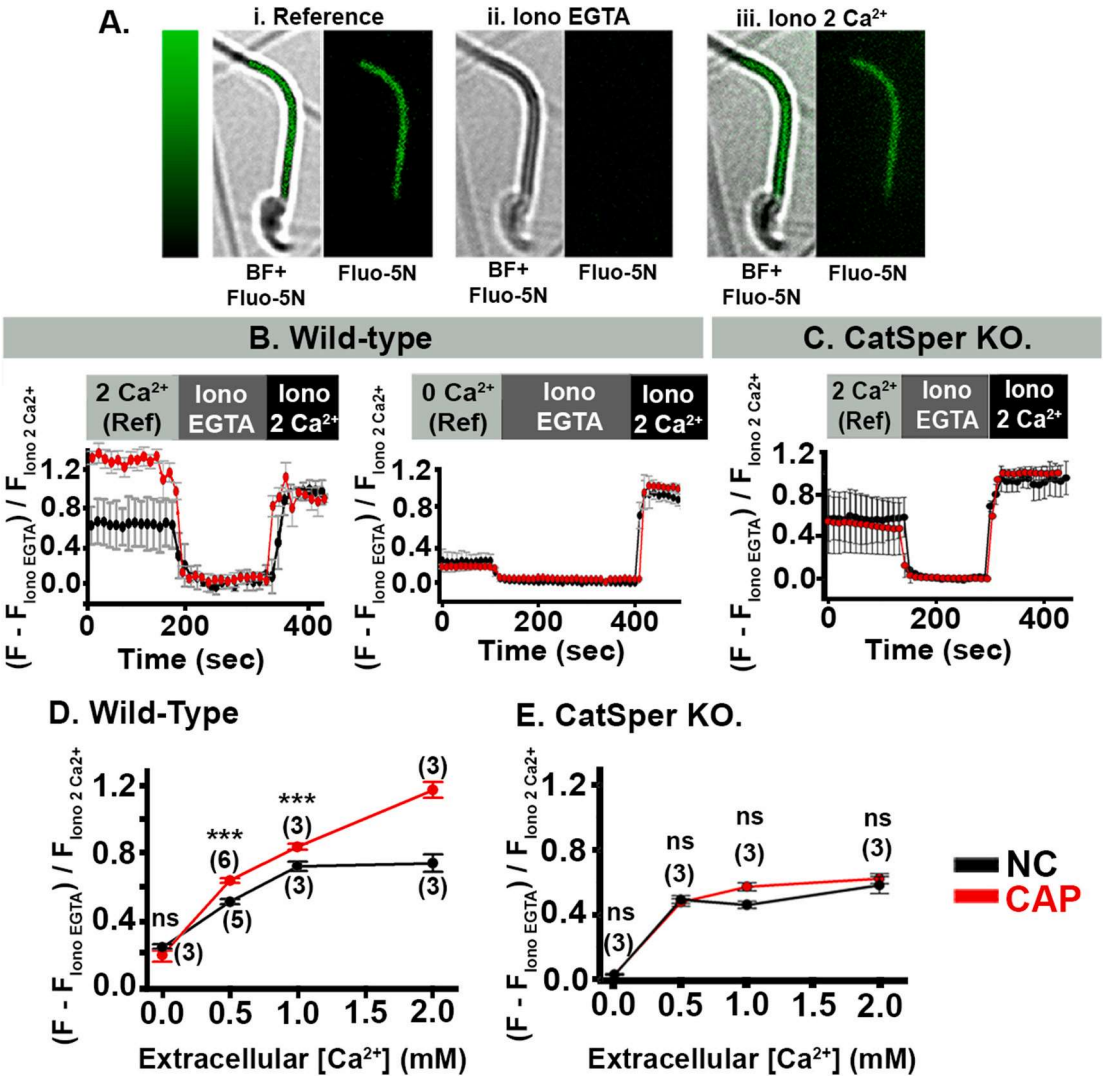


**Fig. 4. Sperm mitochondrial [$Ca^{2+}$] increases during capacitation (CAP) in wild-type, but not in CatSper KO sperm. A.** Representative images of CAP sperm loaded with Fluo-5N; and perfused with i) 2 mM $Ca^{2+}$ (Reference), ii) 0 $Ca^{2+}$ + 2 mM EGTA and Ionomycin (Iono EGTA), iii) Ionomycin +2 mM $Ca^{2+}$ (Iono 2 $Ca^{2+}$). Images in i, ii, iii are on the left: bright field (BF) merged with Fluo-5N fluorescence (FITC). Right, Fluo-5N fluorescence. Color bars represent color code for the gray scale from 0 to 255. B and C, Representative traces of Fluo-5N fluorescence in the sperm midpiece from NC (black) and CAP (red) sperm incubated in 2 mM $Ca^{2+}$ (B, left), and in 0 mM $Ca^{2+}$ (B, right). C. Representative traces of Fluo-5N fluorescence from NC and CAP CatSper KO sperm. D. Normalized values of Fluo-5N fluorescence at reference (ref), in NC and CAP sperm at different extracellular [$Ca^{2+}$]. E. Fluo-5N fluorescence at reference in CatSper KO samples, obtained under NC and CAP conditions, at different extracellular [$Ca^{2+}$]. Statistical significance between CAP and NC samples at each extracellular [$Ca^{2+}$] were evaluated with an independent *t-test*. Fluorescence values are shown in Table 2 ns $p > 0.050$, and ***$p < 0.001$. (n) represents the number of animals. (For interpretation of the references to color in this figure legend, the reader is referred to the Web version of this article.)

**Table 2**
Fluo-5N fluorescent values corresponding to mitochondrial [$Ca^{2+}$] before and after CAP at different extracellular [$Ca^{2+}$]. Fluo-5N fluorescence values were normalized using Ionomycin +0 mM $Ca^{2+}$ + EGTA (Iono EGTA) values and Ionomycin +2 mM $Ca^{2+}$ (Iono 2 $Ca^{2+}$) values. To determine statistical significance between NC and CAP samples at each extracellular [$Ca^{2+}$], independent *t-test* were used.

| Extracellular [$Ca^{2+}$] mM | | Wild-type | | | P-Value | | CatSper KO | | | p-value |
|---|---|---|---|---|---|---|---|---|---|---|
| | | Mean | SD | n | | | Mean | SD | n | |
| **0** | **NC** | 0.2398 | 0.1556 | 3 | **0.197** | **NC** | 0.0201 | 0.0167 | 3 | **0.396** |
| | **CAP** | 0.1935 | 0.1136 | 3 | | **CAP** | 0.0234 | 0.0248 | 3 | |
| **0.5** | **NC** | 0.5122 | 0.2798 | 5 | **0.035** | **NC** | 0.4893 | 0.1984 | 3 | **0.676** |
| | **CAP** | 0.6394 | 0.2413 | 6 | | **CAP** | 0.4717 | 0.1995 | 3 | |
| **1** | **NC** | 0.7242 | 0.2798 | 3 | **0.01** | **NC** | 0.4562 | 0.1649 | 3 | **0.63** |
| | **CAP** | 0.8402 | 0.208 | 3 | | **CAP** | 0.5688 | 0.257 | 3 | |
| **2** | **NC** | 0.7427 | 0.4494 | 3 | **0.022** | **NC** | 0.579 | 0.3106 | 3 | **0.155** |
| | **CAP** | 1.1791 | 0.4635 | 3 | | **CAP** | 0.6194 | 0.3805 | 3 | |

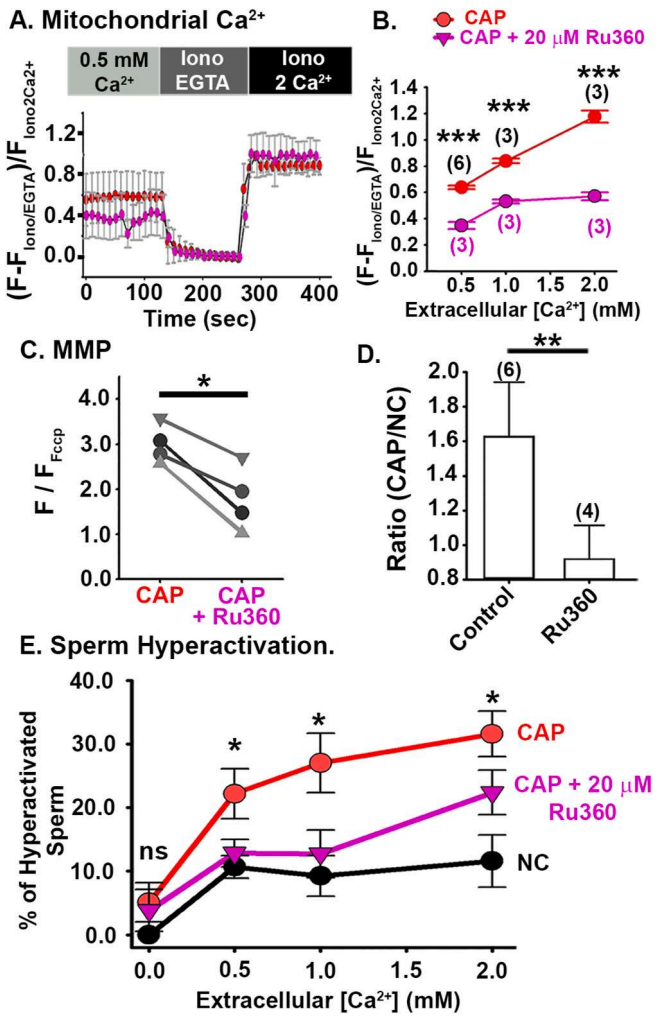


**Fig. 5. Effect of the Mitochondrial Calcium Uniporter inhibitor, Ru360 on mitochondrial [$Ca^{2+}$], mitochondrial function, and sperm hyperactivation. A.** Representative Fluo-5N fluorescence traces from CAP sperm and CAP with Ru360 at 0.5 mM extracellular $Ca^{2+}$. **B.** Normalized Fluo-5N fluorescence in NC and CAP conditions, at different extracellular [$Ca^{2+}$]. Graph shows mean values ± SD of cells responding to Iono EGTA and Iono 2$Ca^{2+}$. An independent *t-test* was used to determined statistical difference. **C.** Normalized TMRM fluorescence under CAP and CAP + Ru360 conditions (n = 4). To determine statistical significance, paired *t-test* were used. **D.** TMRM fluorescence ratio in wild-type sperm, under CAP (control) and CAP + Ru360. To determine statistical significance an independent *t-test* was used. **E.** Percentage of hyperactivated sperm measured by CASA from sperm samples incubated in NC, CAP or CAP +20 μM Ru360 media, at different extracellular [$Ca^{2+}$]. Values are also presented in Table 4. An independent *t-test* were used to evaluate statistical significance between NC, CAP and CAP + Ru360 groups at different [$Ca^{2+}$] (n = 5). Error Bars in figure represent SD. ns $P > 0.050$, *$p < 0.050$, **$p < 0.010$, and ***$p < 0.001$. (n) represents the number of animals.

**Table 3**
**Fluo-5N fluorescence values corresponding to mitochondrial $Ca^{2+}$ from wild-type sperm CAP in the presence of Ru360 at different extracellular [$Ca^{2+}$].** Fluo-5N values were normalized using Ionomycin +0 mM $Ca^{2+}$ + EGTA (Iono EGTA) values and Ionomycin +2 mM $Ca^{2+}$ (Iono 2 $Ca^{2+}$) values.

| Extracellular [$Ca^{2+}$] mM | | Wild-type | | |
|---|---|---|---|---|
| | | Mean | SD | n |
| **0.5** | **CAP + Ru360** | 0.3483 | 0.027 | 3 |
| **1** | **CAP + Ru360** | 0.5324 | 0.015 | 3 |
| **2** | **CAP + Ru360** | 0.5725 | 0.0298 | 3 |

MMP was 5% lower in CAP than NC sperm treated with Ru360 (Fig. 5D). Thus, we concluded that Ru360 abolished the MMP increase observed in wild-type sperm after capacitation.

Finally, we assessed the effects of Ru360 on sperm hyperactivation by performing computer-assisted sperm analysis (CASA). In NC sperm, only 10% of sperm were hyperactive even at the highest extracellular [$Ca^{2+}$] tested (2 mM). In CAP samples treated with vehicle, approximately 30% of sperm were hyperactive at 2 mM extracellular [$Ca^{2+}$]. However, Ru360 treatment significantly diminished capacitation-induced hyperactivation (Fig. 5E and Table 4). To exclude the possibility that Ru360 impaired hyperactivation by directly inhibiting CatSper channels, we used Fluo-4 AM fluorescence to measure $Ca^{2+}$ influx through CatSper channels in the absence and presence of Ru360. We found that membrane depolarization with KCl still triggers an increase of cytoplasmic [$Ca^{2+}$] even in the presence of Ru360, confirming that this compound did not inhibit $Ca^{2+}$ influx through CatSper channels (Supplementary Fig. 7A). Together, these results suggest that the increase in mitochondrial [$Ca^{2+}$] contributes to sperm hyperactivation, and that this increase depends on extracellular [$Ca^{2+}$].

### 3.6. *Hyperactivation relies on ADP/ATP translocase activity*

In Fig. 1B, we showed that the RCR was higher in CAP sperm than in NC sperm, suggesting that mitochondria in CAP sperm produce more ATP, which could be required for sperm hyperactivation. To test this idea, we inhibited ATP/ADP exchange between the mitochondria and the cytosol by capacitating sperm in the presence of Atractyloside (ATR) (an inhibitor of the adenine nucleotide translocase residing in the inner mitochondrial membrane). Measurements with CASA, showed that the percentage of hyperactivated sperm was significantly lower in sperm treated with ATR than in those treated with vehicle (26.57 Mean ± 5.95 SD, n = 10, vs. 34.02 Mean ± 8.77 SD, n = 9, $P < 0.01$, Fig. 6A). To exclude the possibility that ATR impaired hyperactivation by directly inhibiting CatSper, we used Fluo-4 AM fluorescence to measure $Ca^{2+}$ influx through CatSper in the absence and presence of ATR. This experiment confirmed that ATR did not inhibit $Ca^{2+}$ influx through CatSper channels (Supplementary Fig. 7B). It is noteworthy that the percentages of hyperactivity inhibition were very similar when sperm were incubated in the presence of Ru360 or ATR, (35.77 Mean ± 26.85 SD, n = 6, vs. 26.42 Mean ± 10.41 SD, n = 6; Fig. 6B). This result suggests that $Ca^{2+}$ entry into mitochondria during capacitation is important for the ATP production involved in sperm hyperactivation.

**Table 4**
Percentage of hyperactivation from Fig. 5E. Hyperactivated motility was measured with CASA in NC, CAP (Control), and CAP+20 μM Ru360 samples at different [$Ca^{2+}$]. Independent *t-test* was used to evaluate statistical significance between NC, CAP and CAP + Ru360 groups at the same [$Ca^{2+}$].

| Extracellular [$Ca^{2+}$] mM | | Wild-type | | | p-value | |
|---|---|---|---|---|---|---|
| | | Mean | SD | n | | |
| 0 | NC | 0 | 2.50E-03 | 4 | 0.197 | |
| | **CAP** | 5.0865 | 6.1481 | 4 | | **0.91** |
| | **CAP + Ru360** | 3.8123 | 7.3331 | 5 | | |
| **0.5** | **NC** | 10.6899 | 4.3254 | 6 | **0.035** | |
| | **CAP** | 22.1885 | 9.6493 | 6 | | **0.04** |
| | **CAP + Ru360** | 12.85 | 5.283 | 6 | | |
| **1** | **NC** | 9.2572 | 7.7815 | 6 | **0.01** | |
| | **CAP** | 25.8553 | 10.9269 | 7 | | **0.03** |
| | **CAP + Ru360** | 17.4244 | 7.8503 | 7 | | |
| **2** | **NC** | 11.5959 | 9.2466 | 5 | **0.022** | |
| | **CAP** | 28.3665 | 10.678 | 6 | | **0.03** |
| | **CAP + Ru360** | 17.7953 | 10.2253 | 6 | | |

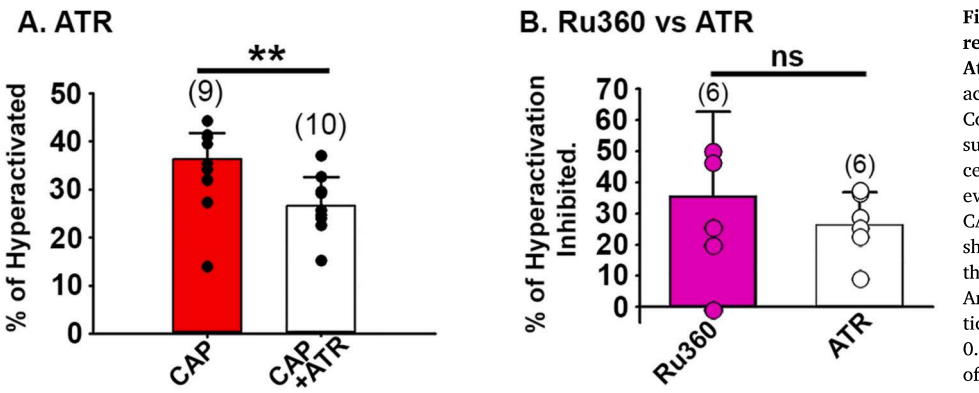


**Fig. 6. Mouse sperm hyperactivation is reduced by ADP/ATP translocase inhibitor Atractyloside (ATR). A.** Percentage of hyperactivated sperm measured by CASA from CAP Control and CAP +5 μM ATR conditions. Measurements were done in media with 2 mM extracellular $Ca^{2+}$. Independent *t-test* was used to evaluate statistical significance between CAP and CAP + ATR. Error Bars represent SD. **B.** Graph shows percentage of hyperactivation inhibited by the presence of Ru360 or ATR during capacitation. An independent *t-test* was used to evaluate statistical significance. Error Bars represent SD. ns $p > 0.050$, and $^{**}p < 0.010$. (n) represents the number of animals.

## 4. Discussion

Together, our data support the following model (Fig. 7): CatSper channel activation during sperm capacitation induces $Ca^{2+}$ influx and an increase in cytoplasmic [$Ca^{2+}$]. This increase in intracellular [$Ca^{2+}$] starts in the principal piece, propagates through the midpiece, and reaches the head in a few seconds [15]. The MCU then transports $Ca^{2+}$ into the mitochondria, leading to increased mitochondrial efficiency, which promotes sperm hyperactivation and sperm's ability to fertilize an oocyte.

The role of mitochondria in mammalian sperm function, quality, and fertilization ability has been intensely debated for several years [12,14,25,26,35]. The contribution of mitochondria to sperm bioenergetics is unclear, and the source of the ATP used for sperm motility and hyperactivation has been long debated. The studies carried out in several species have provided different or conflicting results. In mouse sperm, glycolysis-produced ATP is sufficient to sustain progressive motility [12,27]. Conversely, in human sperm, a strong correlation has been noted between mitochondrial functionality and sperm motility or overall quality [28,29]. Therefore, one idea is that sperm have versatile metabolism, allowing them to use species or environment dependent mechanisms for energy production [29,30].

Here, we measured mitochondrial activity in NC and CAP mouse sperm by two independent methods. First, we used HRR to measure mitochondrial oxygen consumption in intact and motile sperm cells [16,31,32]. During capacitation, mitochondrial coupling efficiency increased, indicating that mitochondrial electron transport chain is more closely coupled to ADP phosphorylation in CAP sperm than in NC sperm. Additionally, we noted an increase in RCR in CAP sperm, suggesting that mitochondrial function improved to increase ATP production, or to maintain the elevated MMP. However, the reserve respiratory capacity, which reflects the capacity of sperm to respond to energy demands, was not modified in CAP sperm, suggesting that sperm operate close to their bioenergetic limit [17]. As a second method to study mitochondrial function, we used the voltage-sensitive dye TMRM to measure sperm MMP both at the sperm population, and single cell level, observing an increase in MMP and mitochondria function [33]. Therefore, we conclude that sperm mitochondrial function increases during capacitation.

Our work has a significant advantage over previous findings

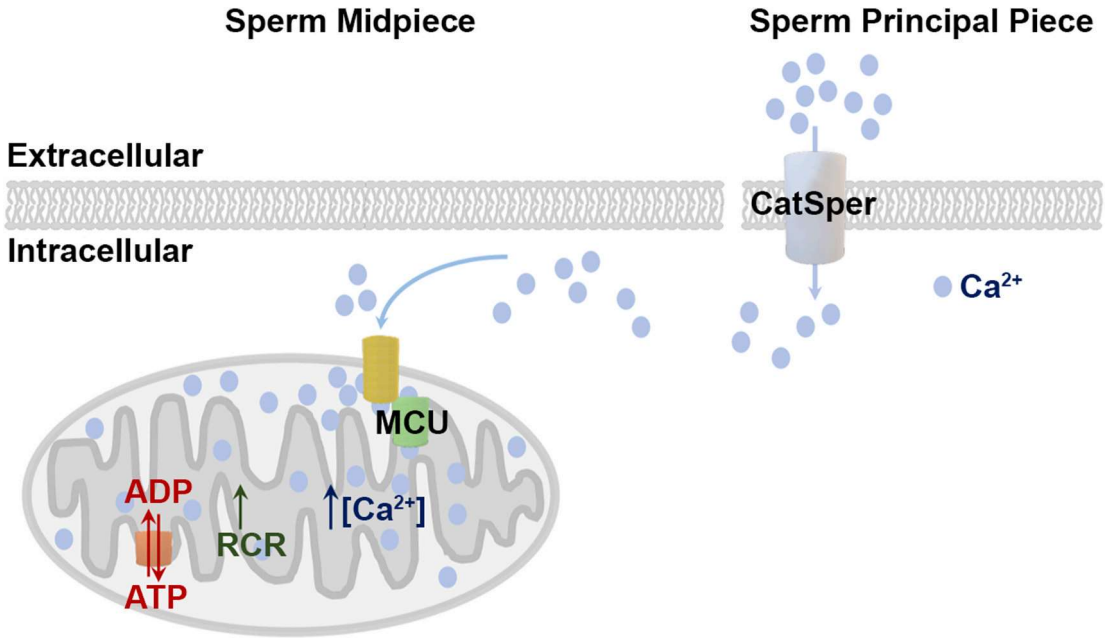


**Fig. 7. Proposed model for a role of sperm mitochondria in capacitation/hyperactivation processes.** CatSper activation during capacitation determines $Ca^{2+}$ influx and the increase in cytoplasmic [$Ca^{2+}$], that starts in the sperm principal piece, propagates through the midpiece, and reaches the head in a few seconds (20). Our data shows that the $Ca^{2+}$ propagation through the midpiece leads to an increase in mitochondrial $Ca^{2+}$ mediated by MCU. The increase in mitochondrial $Ca^{2+}$ translates into an increase in mitochondrial efficiency that in turn promotes hyperactivation and *in-vitro* fertilization. Other molecular mechanisms involved in this pathway (e. g. possible role of the redundant nuclear envelop) need to be elucidated.

regarding a role of mitochondria in sperm capacitation. Our study was conducted in intact and motile sperm, while earlier studies have used non-physiological conditions (permeabilized and/or non-motile sperm) [13,14,34–36] .

Our experiments done in the presence of mitochondrial function inhibitors indicated that mitochondrial activity is not necessary for two features of capacitation –AR and tyrosine phosphorylation– but is contributing significantly to sperm hyperactivation and fertilization ability. These findings are consistent with observations that sperm from CatSper KO mice fail to hyperactivate and fertilize, but the AR and tyrosine phosphorylation are unaffected [37]. Additionally, these findings are consistent with our observation that sperm from CatSper KO mice did not have an increase in RCR or MMP in capacitating conditions. Although the downstream targets of the CatSper-mediated cytoplasmic [$Ca^{2+}$] increase have not been fully characterized [6,7], sperm from CatSper KO have decreased NADH levels in the midpiece and a deficit in ATP production [5,37]. It is possible that the tail-to-head propagation of $Ca^{2+}$ initiated by CatSper activation triggers an increase in [NAD] and may regulate ATP homeostasis [15]. Moreover, our finding that CatSper channels are required for increased mitochondrial [$Ca^{2+}$] in CAP sperm adds a new role for the sperm-specific $Ca^{2+}$ channel.

Several lines of evidence suggest that, at least in somatic cells, regulated $Ca^{2+}$ entry into mitochondria increases the efficiency of oxidative respiration [38,39]. Mitochondrial [$Ca^{2+}$] is considered a central regulator of oxidative phosphorylation by mediating NADH production and controlling activity of pyruvate dehydrogenase, isocitrate dehydrogenase, and α-ketoglutarate dehydrogenase [8,40]. Mitochondrial [$Ca^{2+}$] also plays an important role in regulating ATP synthase [8,39,41] and can trigger the release of pro-apoptotic agents by the mitochondria [42]. However, the precise role of $Ca^{2+}$ in sperm mitochondria is still under debate [11]. Some evidence suggests that maintenance of mitochondrial $Ca^{2+}$ homoeostasis is essential for motility regulation in human sperm [43] and bovine sperm [44,45]. Whereas in contrast, other studies reported that sperm mitochondrial [$Ca^{2+}$] is unaltered by mitochondrial uncoupling [46] and in bulls, mitochondrial activity in hyperactivated sperm appears not to be regulated by [$Ca^{2+}$] [47]. Thus, the role of $Ca^{2+}$ in sperm mitochondrial $Ca^{2+}$ homoeostasis may be species-specific.

Our data showing that mitochondrial $Ca^{2+}$ uptake in mouse sperm occurs through the MCU are consistent with similar findings in somatic cells where MCU is known to control intracellular $Ca^{2+}$ signals, cell metabolism, and cell survival [9,48]. Specifically, we found that the MCU inhibitor Ru360 decreased mitochondrial [$Ca^{2+}$] in mouse sperm during capacitation and inhibited sperm hyperactivation. These results agree with previous results showing that mitochondrial $Ca^{2+}$ contributes to motility regulation in human sperm [43] and capacitation in bovine sperm [45]. Proteomic studies have confirmed that human sperm possess both MCU and MCU regulator 1 [11,49], so this protein may be required for mitochondrial $Ca^{2+}$ uptake in human sperm as well. MCU has a low affinity for $Ca^{2+}$ uptake [9,54], leading some to speculate that $Ca^{2+}$ transfer into mitochondria occurs at highly specialized regions of close contact between mitochondria and endoplasmic reticulum called mitochondria-associated membranes [9]. Some of the molecular components of mitochondria-associated membranes are present in sperm, distributed in the acrosome and at the sperm neck and anterior midpiece. Endoplasmic reticulum in this location is referred to as the redundant nuclear envelope [47,51]. Further studies are needed to determine whether these sites of contact between the redundant nuclear envelope and mitochondria participate in the increase of mitochondrial [$Ca^{2+}$] during capacitation.

In conclusion, our results show that mitochondrial activity (i.e., oxygen consumption, generation of the electrochemical gradient, ATP/ADP exchange) increases during sperm capacitation and this increase in activity contributes to sperm hyperactivation and sperm fertilization. The increase in mitochondrial coupling efficiency is consistent with $Ca^{2+}$ influx through CatSper channels and $Ca^{2+}$ entry into the mitochondria through the MCU. This increase in mitochondrial $Ca^{2+}$ could translate either into an increase in ATP production due to the $Ca^{2+}$ dependency of many of the mitochondrial enzymes, or play a role in shaping intracellular calcium signals. Both mechanisms, acting independently or together, would be relevant to achieve sperm hyperactivation. Our discovery of new mechanisms that explain sperm function may lead to the use of new molecules for fertility treatments and male contraception.

## Declaration of competing interest

The authors declare no conflict of Interest.

## Acknowledgements

We thank Dr. Deborah Frank for the critical review of the manuscript, as well as Dr. Emily Hunter and Nathan Pomper for the editing assistance provided through InPrint: A Scientific Editing Network at Washington University in St. Louis. We thank Dr. Lis Puga Molina for her assistance with the CASA experiments. We also thank Dr. Valeria Valez, from CEINBIO-UdelaR, for assistance with figures design.

## Appendix A. Supplementary data

Supplementary data to this article can be found online at https://doi.org/10.1016/j.redox.2021.102176.

## Funding and financial

RR and AC are supported by grants from Universidad de la República (CSIC_2018 , Espacio Interdisciplinario_2019). Additional funding was obtained from the Programa de Desarrollo de Ciencias Básicas (PEDECIBA, Uruguay). PI, SP, MF and RS are supported from Universidad de la República (I + D, CSIC 2014, (I + D, CSIC 2016 and FMV_1_2017_1_136490 ANII- Uruguay).

CMS funding from NIH grant RO1 HD069631 and LEAP grant Award, Washington University in Saint Louis.

## References

[1] C.R. Austin, The "capacitation" of the mammalian sperm, Nature 170 (1952) 326.
[2] M.C. Chang, Fertilizing capacity of spermatozoa deposited into the fallopian tubes, Nature 168 (4277) (1951) 697–698.
[3] J. Correia, F. Michelangeli, S. Publicover, Regulation and roles of Ca2+ stores in human sperm, Reproduction 150 (2) (2015) R65–R76.
[4] P.V. Lishko, N. Mannowetz, CatSper: a unique calcium channel of the sperm flagellum, Current Opinion in Physiology 2 (2018) 109–113.
[5] D. Ren, B. Navarro, G. Perez, A.C. Jackson, S. Hsu, Q. Shi, J.L. Tilly, D.E. Clapham, A sperm ion channel required for sperm motility and male fertility, Nature 413 (6856) (2001) 603–609.
[6] R. Rahban, S. Nef, CatSper: the complex main gate of calcium entry in mammalian spermatozoa, Mol. Cell. Endocrinol. (2020) 110951.
[7] L. Vyklicka, P.V. Lishko, Dissecting the signaling pathways involved in the function of sperm flagellum, Curr. Opin. Cell Biol. 63 (2020) 154–161.
[8] J.G. McCormack, A.P. Halestrap, R.M. Denton, Role of calcium ions in regulation of mammalian intramitochondrial metabolism, Physiol. Rev. 70 (2) (1990) 391–425.
[9] R. Rizzuto, D. De Stefani, A. Raffaello, C. Mammucari, Mitochondria as sensors and regulators of calcium signalling, Nat. Rev. Mol. Cell Biol. 13 (9) (2012) 566–578.
[10] R. Bravo-Sagua, V. Parra, C. López-Crisosto, P. Díaz, A.F.G. Quest, S. Lavandero, Calcium transport and signaling in mitochondria, Comprehensive Physiology 7 (2) (2017) 623–634.
[11] A. Amaral, B. Lourenço, M. Marques, J. Ramalho-Santos, Mitochondria functionality and sperm quality, Reproduction 146 (5) (2013) R163–R174.
[12] K. Miki, W. Qu, E.H. Goulding, W.D. Willis, D.O. Bunch, L.F. Strader, S. D. Perreault, E.M. Eddy, D.A. O'Brien, Glyceraldehyde 3-phosphate dehydrogenase-S, a sperm-specific glycolytic enzyme, is required for sperm motility and male fertility, Proc. Natl. Acad. Sci. U.S.A. 101 (47) (2004) 16501–16506.
[13] A. Ferramosca, V. Zara, Bioenergetics of mammalian sperm capacitation, BioMed Res. Int. 2014 (2014) 902953.
[14] A. Stendardi, R. Focarelli, P. Piomboni, D. Palumberi, F. Serafini, A. Ferramosca, V. Zara, Evaluation of mitochondrial respiratory efficiency during in vitro capacitation of human spermatozoa, Int. J. Androl. 34 (3) (2011) 247–255.

[15] J. Xia, D. Reigada, C.H. Mitchell, D. Ren, CATSPER channel-mediated Ca2+ entry into mouse sperm triggers a tail-to-head propagation, Biol. Reprod. 77 (3) (2007) 551–559.

[16] A. Cassina, P. Silveira, L. Cantu, J.M. Montes, R. Radi, R. Sapiro, Defective human sperm cells are associated with mitochondrial dysfunction and oxidant production, Biol. Reprod. 93 (5) (2015) 119.

[17] M.D. Brand, D.G. Nicholls, Assessing mitochondrial dysfunction in cells, Biochem. J. 435 (2) (2011) 297–312.

[18] P. Uribe, J.V. Villegas, R. Boguen, F. Treulen, R. Sánchez, P. Mallmann, V. Isachenko, G. Rahimi, E. Isachenko, Use of the fluorescent dye tetramethylrhodamine methyl ester perchlorate for mitochondrial membrane potential assessment in human spermatozoa, Andrologia 49 (9) (2017).

[19] Q. Yang, Y. Wen, L. Wang, Z. Peng, R. Yeerken, L. Zhen, P. Li, X. Li, Ca2+ ionophore A23187 inhibits ATP generation reducing mouse sperm motility and PKA-dependent phosphorylation, Tissue Cell 66 (2020) 101381.

[20] S. Creed, M. McKenzie, in: M. Haznadar (Ed.), Measurement of Mitochondrial Membrane Potential with the Fluorescent Dye Tetramethylrhodamine Methyl Ester (TMRM) BT - Cancer Metabolism: Methods and Protocols, Springer, New York, 2019, pp. 69–76.

[21] A.A. Kabbara, D.G. Allen, The use of the indicator flou-5N to measure sarcoplasmic reticulum calcium in single muscle fibres of the cane toad, J. Physiol. (2001).

[22] P.E. Visconti, J.L. Bailey, G.D. Moore, D. Pan, P. Olds-Clarke, G.S. Kopf, 47. Capacitation of mouse spermatozoa. I. Correlation between the capacitation state and protein tyrosine phosphorylation, Development 121 (4) (1995) 1129–1137.

[23] T. Pathak, M. Trebak, Mitochondrial Ca2+ signaling, in: Pharmacology and Therapeutics, 2018.

[24] Y. Kirichok, G. Krapivinsky, D.E. Clapham, The mitochondrial calcium uniporter is a highly selective ion channel, Nature 427 (6972) (2004) 360–364.

[25] S.G. Goodson, Y. Qiu, K.A. Sutton, G. Xie, W. Jia, D.A. O'Brien, Metabolic substrates exhibit differential effects on functional parameters of mouse sperm capacitation, Biol. Reprod. 87 (3) (2012) 75.

[26] J.M. Nascimento, L.Z. Shi, J. Tam, C. Chandsawangbhuwana, B. Durrant, E. L. Botvinick, M.W. Berns, Comparison of glycolysis and oxidative phosphorylation as energy sources for mammalian sperm motility, using the combination of fluorescence imaging, laser tweezers, and real-time automated tracking and trapping, J. Cell. Physiol. 217 (3) (2008) 745–751.

[27] C. Mukai, M. Okuno, Glycolysis plays a major role for adenosine triphosphate supplementation in mouse sperm flagellar movement, Biol. Reprod. 71 (2) (2004) 540–547.

[28] F. Gallon, C. Marchetti, N. Jouy, P. Marchetti, The functionality of mitochondria differentiates human spermatozoa with high and low fertilizing capability, Fertil. Steril. 86 (5) (2006) 1526–1530.

[29] E. Ruiz-Pesini, C. Diez, A.C. Lapeña, A. Pérez-Martos, J. Montoya, E. Alvarez, J. Arenas, M.J. López-Pérez, Correlation of sperm motility with mitochondrial enzymatic activities, Clin. Chem. 44 (8 Pt 1) (1998) 1616–1620.

[30] B.T. Storey, Mammalian sperm metabolism: oxygen and sugar, friend and foe, Int. J. Dev. Biol. 52 (5–6) (2008) 427–437.

[31] C.R. Darr, G.A. Cortopassi, S. Datta, D.D. Varner, S.A. Meyers, Mitochondrial oxygen consumption is a unique indicator of stallion spermatozoal health and varies with cryopreservation media, Theriogenology (2016).

[32] C.R. Moraes, S. Meyers, The sperm mitochondrion: organelle of many functions, in: Animal Reproduction Science, 2018.

[33] N. Moscatelli, B. Spagnolo, M. Pisanello, E.D. Lemma, M. De Vittorio, V. Zara, F. Pisanello, A. Ferramosca, Single-cell-based evaluation of sperm progressive motility via fluorescent assessment of mitochondria membrane potential, Sci. Rep. 7 (1) (2017) 17931.

[34] M. Balbach, J. Buck, L.R. Levin, Using an extracellular flux analyzer to measure changes in glycolysis and oxidative phosphorylation during mouse sperm capacitation, JoVE (2020).

[35] M. Balbach, M.G. Gervasi, D.M. Hidalgo, P.E. Visconti, L.R. Levin, J. Buck, Metabolic changes in mouse sperm during capacitation, Biol. Reprod. 103 (4) (2020) 791–801.

[36] A. Ferramosca, R. Focarelli, P. Piomboni, L. Coppola, V. Zara, Oxygen uptake by mitochondria in demembranated human spermatozoa: a reliable tool for the evaluation of sperm respiratory efficiency, Int. J. Androl. 31 (3) (2008) 337–345.

[37] T.A. Quill, S.A. Sugden, K.L. Rossi, L.K. Doolittle, R.E. Hammer, D.L. Garbers, Hyperactivated sperm motility driven by CatSper2 is required for fertilization, Proc. Natl. Acad. Sci. U.S.A. 100 (25) (2003) 14869–14874.

[38] S. Cortassa, M.A. Aon, E. Marbán, R.L. Winslow, B. O'Rourke, An integrated model of cardiac mitochondrial energy metabolism and calcium dynamics, Biophys. J. 84 (4) (2003) 2734–2755.

[39] J.G. McCormack, R.M. Denton, The role of intramitochondrial Ca2+ in the regulation of oxidative phosphorylation in mammalian tissues, Biochem. Soc. Trans. 21 (Pt 3) (1993) 793–799, 3.

[40] J.G. McCormack, R.M. Denton, Mitochondrial Ca2+ transport and the role of intramitochondrial Ca2+ in the regulation of energy metabolism, Dev. Neurosci. 15 (3–5) (1993) 165–173.

[41] P.R. Territo, S.A. French, M.C. Dunleavy, F.J. Evans, Calcium activation of heart mitochondrial oxidative phosphorylation: RAPID kinetics OFmV O2, NADH, and light scattering, J. Biol. (Bronx N Y) (2001). https://www.jbc.org/article/S0021-9258(18)46605-7/abstract.

[42] G. Szalai, R. Krishnamurthy, G. Hajnóczky, Apoptosis driven by IP(3)-linked mitochondrial calcium signals, EMBO J. 18 (22) (1999) 6349–6361.

[43] A. Bravo, F. Treulen, P. Uribe, R. Boguen, R. Felmer, J.V. Villegas, Effect of mitochondrial calcium uniporter blocking on human spermatozoa, Andrologia 47 (6) (2015) 662–668.

[44] S. Meyers, E. Bulkeley, A. Foutouhi, Sperm mitochondrial regulation in motility and fertility in horses, Reproduction in Domestic Animals = Zuchthygiene 54 (Suppl 3) (2019) 22–28.

[45] P.C. Rodriguez, M.M. Satorre, M.T. Beconi, Effect of two intracellular calcium modulators on sperm motility and heparin-induced capacitation in cryopreserved bovine spermatozoa, Anim. Reprod. Sci. 131 (3–4) (2012) 135–142.

[46] G. Machado-Oliveira, L. Lefièvre, C. Ford, M.B. Herrero, C. Barratt, T.J. Connolly, K. Nash, A. Morales-Garcia, J. Kirkman-Brown, S. Publicover, Mobilisation of Ca2+ stores and flagellar regulation in human sperm by S-nitrosylation: a role for NO synthesised in the female reproductive tract, Development 135 (22) (2008) 3677–3686.

[47] H.-C. Ho, S.S. Suarez, Characterization of the intracellular calcium store at the base of the sperm flagellum that regulates hyperactivated motility, Biol. Reprod. 68 (5) (2003) 1590–1596.

[48] M. Patron, A. Raffaello, V. Granatiero, A. Tosatto, G. Merli, D. De Stefani, L. Wright, G. Pallafacchina, A. Terrin, C. Mammucari, R. Rizzuto, The mitochondrial calcium uniporter (MCU): molecular identity and physiological roles, J. Biol. Chem. 288 (15) (2013) 10750–10758.

[49] H. Wang, X. Cheng, J. Tian, Y. Xiao, T. Tian, F. Xu, X. Hong, M.X. Zhu, TRPC channels: structure, function, regulation and recent advances in small molecular probes, Pharmacol. Therapeut. 209 (2020) 107497.

[51] K. Ho, C.A. Wolff, S.S. Suarez, CatSper-null mutant spermatozoa are unable to ascend beyond the oviductal reservoir, Reprod. Fertil. Dev. 21 (2) (2009) 345–350.

[52] M.M. Bradford, A rapid and sensitive method for the quantitation of microgram quantities of protein utilizing the principle of protein-dye binding, Anal. Biochem. 72 (1) (1976) 248–254. https://doi.org/10.1016/0003-2697(76)90527-3.

[54] P. Wang, C. Fernandez-Sanz, W. Wang, S.-S. Sheu, Why don't mice lacking the mitochondrial Ca2+ uniporter experience an energy crisis? J. Physiol. 598 (7) (2020) 1307–1326.

[55] Julio Chavez Cesar, et al., SLO3 K+ channels control calcium entry through CATSPER channels in sperm, J.Biol Chem 289 (46) (2014).